

IMECE2005-81217

**RESPONSE OF MEMS DEVICES UNDER SHOCK LOADS**

Mohammad I. Younis

Dept of Mechanical Engineering,  
State University of New York at BinghamtonBinghamton, New York 13902,  
Email: myounis@binghamton.edu

Ronald Miles

Dept of Mechanical Engineering,  
State University of New York at BinghamtonBinghamton, New York 13902,  
Email: miles@binghamton.edu**ABSTRACT**

There is strong experimental evidence for the existence of strange modes of failure of MEMS devices under shock. Such failures have not been explained with conventional models of MEMS. These failures are characterized by overlaps between moving microstructures and stationary electrodes, which cause electrical shorts. This work presents a model and simulation of MEMS devices under the combination of shock loads and electric actuation, which will shed the light on the influence of these forces on the pull-in instability. Our results indicate that the reported strange failures can be attributed to early dynamic pull-in instability. The results show that the combination of a shock load and an electric actuation makes the instability threshold much lower than the threshold predicted considering the effect of shock alone or electric actuation alone. Several results are presented showing the response of MEMS devices due to half-sine pulse, triangle pulse, and rectangular pulse shock loads of various durations and strengths. The effects of linear viscous damping and incompressible squeeze-film damping are also investigated.

**INTRODUCTION AND BACKGROUND**

The technology of microelectromechanical systems (MEMS) is now rapidly maturing and many MEMS devices are ready for marketing. Currently, the commercialization of MEMS is a major focus for engineers. One of the most critical issues affecting the commercialization of MEMS devices is their reliability under mechanical shock and impact. MEMS can be exposed to shock during fabrication, deployment, and operation. Examples of such conditions are dynamic loading in space applications and harsh environments in military applications [1]. Further, a crucial criterion for automotive and

industrial applications is the survivability of portable devices containing MEMS when dropped on hard surfaces [2], which can induce significant shock loads. Such highly dynamic loads may lead to various damage mechanisms, such as forming of cracks and chipping of small fragments. Hence, there are increasing demands to improve the design of MEMS to withstand shock loads.

MEMS devices typically employ capacitive sensing and/or actuation, in which one plate or electrode is actuated electrically and its motion is detected by capacitive changes. Electric actuation is the most used and preferred method of excitation and detection in MEMS for its simplicity, high efficiency, and low power consumption. There are numerous examples of MEMS devices, which rely on electric excitation and detection, such as comb-drive actuators, resonant microsensors, and RF MEMS switches. In this method, the driving load is simply the attractive force between two electrodes of a capacitor. The DC component applies an electrostatic force on the structure, thereby deflecting it to a new equilibrium position, while the AC component vibrates the structure around this equilibrium position. The combined electric load has an upper limit beyond which the mechanical restoring force of the structure can no longer resist its opposing electric force, thereby leading to the collapse of the structure. This structural instability phenomenon is known as 'pull-in'. A key aim in the design of many MEMS devices is to tune the electric load away from the pull-in instability, in order to avoid failure of the device.

Many studies have addressed the pull-in phenomenon and presented tools to predict its occurrence so that designers can avoid it [3-6]. However, these studies typically account for the

DC forces only (static analysis). Hence, they do not account for the transient motion of microstructures. Therefore, the possibility of a dynamic instability (i.e., dynamic pull-in) is very high, which can take place below the predicted static instability limit. The dynamic pull-in phenomenon was reported and analyzed for switches actuated by a step voltage [7,8] and with various ramping rates [7]. Both studies indicate that the dynamic pull-in voltage can be as low as 92% of the static pull-in voltage. In the case of AC harmonic excitation, dynamic pull-in was found to be below 50% of the static pull-in voltage [9]. These studies raise the possibility that under the combination of electrical and mechanical shock or impact load, dynamic pull-in may be triggered at even lower values of the applied voltage.

### SHOCK RESPONSE

Structures, including MEMS devices, can be subjected to large forces applied suddenly and over a short period of time relative to the natural period of the structure. These forces are known as mechanical shocks. Shocks can cause damage due to severe vibration of the devices, which may lead to mechanical and/or electrical failure. A shock pulse is characterized by its maximum value, duration, and shape. An actual shock pulse has an irregular shape. However, for modeling and analysis purposes, actual shock pulses can be approximated by simple regular shape pulses. Examples of such pulses are shown in Figure 1.

The response of a system to shock loads can be determined by calculating the shock response spectrum (frequency domain approach) or by calculating the time history of the system (time domain approach). In the first approach, the interest primarily lays in determining the steady-state maximum response of the system to a given shock pulse. The shock response spectrum is a plot of this maximum response for various natural frequencies of the system. This approach has significant benefits from a design point of view because it allows designers to design their device to have a natural frequency corresponding to low shock response. In the time-history approach, the system's equations of motion are integrated with respect to time to determine the transient response as well as the steady-state response when carried out over a long period of time. In this paper, we will use the latter approach due to the importance of the transient behavior on the stability of electrically actuated MEMS.

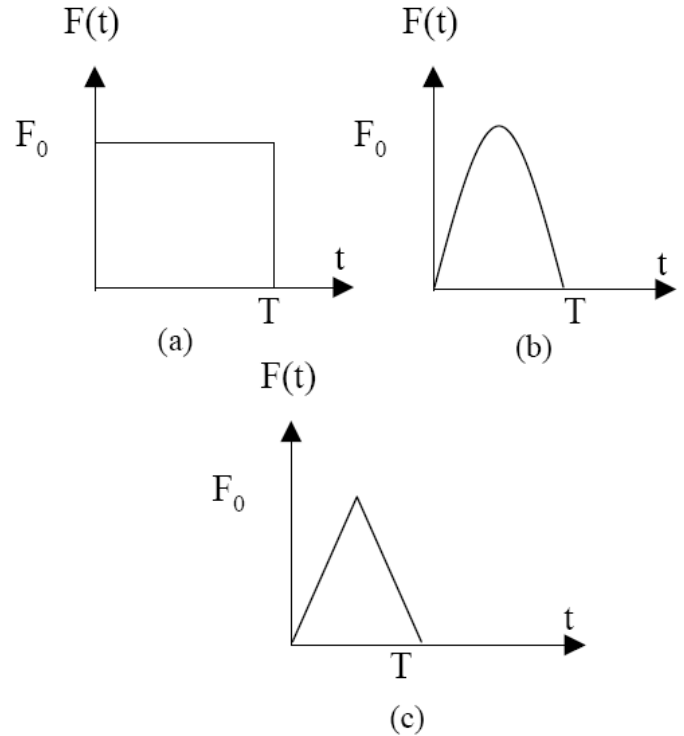


**Figure 1.** Schematic of simple shock pulses used to model actual shock loads. Shown in the figure are (a) the rectangular pulse, (b) the half-sine pulse, and (c) the triangular pulse.

### LITERATURE REVIEW

The reliability of MEMS when exposed to shock and impact has been a subject of increasing interest in recent years. Next, we summarize some of the key papers. Cunningham et al. [10] investigated the effect of stress concentration on the robustness of silicon microstructures against shock. They calculated the stress distribution in microstructures of six different designs using finite-element models. They tested these microstructures experimentally by subjecting them to shock loads of various strengths. They concluded that microstructures with improved stress-concentration areas had the lowest rate of failure. Brown and Davis [11] presented a description of dynamic loading on sensors and techniques used to mitigate failures against high-g shock during ground and flight tests. Lim et al. [12] investigated the effects of shock on a MEMS microactuator integrated with a Head Gimbal Assembly. They used the finite element package ANSYS/LS-DYNA for the modeling and simulation. Yee et al. [13] characterized and tested ferromagnetic micromechanical magnetometers against shock resistance. Beliveau et al. [14] evaluated the performance of three commercial MEMS-based capacitive accelerometers against a high-g shock level, which is higher than their operating range, and compared their performance.

Li and Shemansky [15] studied analytically and experimentally the motion of MEMS accelerometers during drop tests. Two models were used: a simple single-degree-of-

freedom oscillator, consisting of a mass, a spring, and a dashpot and a continuous system beam model to account for the flexibility of the structures. No electric actuation was accounted for in either model. For both models, Li and Shemansky [15] solved analytically the equation of motion for the maximum deflection. Then they calculated the equivalent acceleration that would cause this deflection without a drop test. They found that this acceleration is very large (in the order of tens of thousands of  $g$ ). They verified the analytical solutions by comparing the results to those obtained from the direct integration for the equation of motion. Then, they conducted drop tests on MEMS accelerometers and observed overlap failures between the moving part and the stationary parts, which is caused by the large deflection of the structures during test. They concluded that mechanical constraints have to be imposed on the motion of microstructures to prevent large deflections during impacts and severe dynamic loads.

Wagner et al. [2] studied the response of a MEMS accelerometer to a shock load induced by a drop test. They used a beam theory, for rough estimations, and finite-element analysis to calculate the stress history of the device during impact. They conducted drop-test experiments to assess their finite element results and relate them to the failure mechanism on microstructures. Srikar and Senturia [16] studied the mechanical response of shock-loaded MEMS devices. They modeled MEMS devices as microstructures attached to substrates. They identified three key time scales for the response of microstructures during impact: the acoustic transit time, the time period of vibrations, and the duration of the applied shock load. They indicated that for many MEMS devices and shock conditions, the substrate can be assumed to be a rigid body and it is expected that it will resist stress-wave induced failures. They modeled microstructures as undamped resonators attached to an accelerating base. Coster et al. [17] modeled the performance of an RF MEMS switch actuated by electrostatic force and subjected to shock using a single-degree-of-freedom system. They used a Simulink model to integrate the equation of motion numerically. They simulated the performance of the switch to minimize the insertion loss for various shock amplitudes and applied DC voltages.

Tanner et al. [18] tested MEMS microengines against shock pulses of various time durations and maximum amplitudes. The microengines employ comb-drive actuators, which are composed of folded springs, anchors and a series of comb fingers actuated by electrostatic forces. Tanner et al. [18] observed a strange failure mode in the comb-drive actuators, where the comb fingers contact the ground plane resulting in electrical shorts. They calculated the maximum deflection of a comb finger at the shock level at which this strange failure mode was observed. They found that the force from the shock is much smaller than the force needed to bend the comb finger to touch the ground. Based on this, they concluded that this failure is not related to shock.

From the aforementioned review, we note that much of the conducted research in this field is based on post-failure observation of experimental work. Few theoretical studies have been presented. These highlighted the importance to model, simulate, and characterize the performance of MEMS devices against shock at early stages of design to improve on these designs for an enhanced reliability. There is a need for more extensive modeling and simulation to explain many of the strange failure modes in MEMS microstructures, which were reported in the literature.

## SINGLE-DEGREE-OF-FREEDOM MODEL

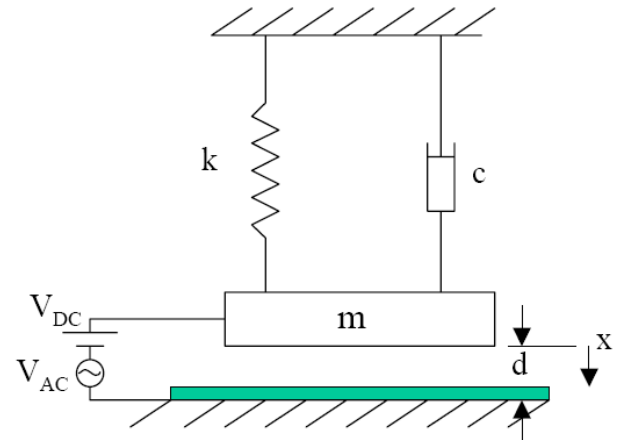


**Figure 2.** Schematic of a single-degree-of-freedom model of a MEMS device.

We use a single-degree-of-freedom model depicted in Figure 2 to represent a MEMS device employing electric actuation and subjected to a shock force  $F_{sh}$ . The device has a moving microstructure of mass  $m$ , which forms one side of a variable capacitor. We use a viscous damper of coefficient  $c$  to model energy dissipation and a spring of coefficient  $k$  to model the effective stiffness of the microstructure, which is due to the elastic restoring force, residual stresses, and the electrostatic force. The equation of motion of the microstructure can be written as

$$m\ddot{x} + c(x)\dot{x} + kx = \frac{\epsilon A [V_{DC} + V_{AC} \cos(\Omega t)]^2}{2(d-x)^2} + F_{sh} \quad (1)$$

where  $x$  is the microstructure deflection,  $V_{DC}$  is the DC polarization voltage,  $V_{AC}$  and  $\Omega$  are the amplitude and frequency of the AC voltage,  $A$  is the area of the microstructure cross section,  $d$  is the capacitor gap width, and  $\epsilon$  is the dielectric constant of the gap medium. Here we assume complete overlapping between the two electrodes of the capacitor. To model the shock force, we use rectangular, half-sine, and triangular pulses shown in Figure 1, which can be expressed respectively as

$$F_{sh} = F_0 \left\{ \sin\left(\frac{\pi}{T}t\right)u(t) + \sin\left[\frac{\pi}{T}(t-T)\right]u(t-T) \right\} \quad (2)$$

$$F_{sh} = \frac{2F_0}{T} [r(t) - 2r(t-T/2) + r(t-T)] \quad (3)$$

$$F_{sh} = F_0 [u(t) - u(t-T)] \quad (4)$$

where  $F_0$  is the maximum shock amplitude,  $T$  is the shock duration,  $u(t)$  is the unit step function, and  $r(t)$  is the unit ramp function.

## RESULTS

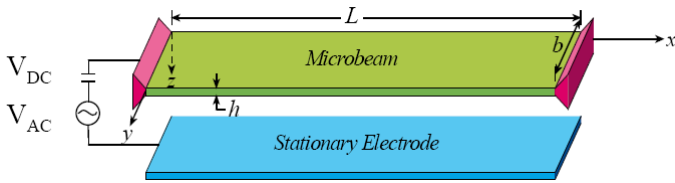


**Figure 3.** Schematic of a resonant sensor microbeam.

We consider a microbeam, Figure 3, employed as a resonant sensor [3], with  $L=510 \mu m$ ,  $h = 1.5 \mu m$ ,  $b = 100 \mu m$ , and  $d = 1.18 \mu m$ . According to the static analysis [5,6], the pull-in voltage for this microbeam is  $V_{DC} \approx 4.4 V$ . We use this value and the equation of the pull-in voltage for a simple spring-mass system [19] to calculate the stiffness constant  $k$ . We assume here, and for rest of the paper, no AC voltage ( $V_{AC} = 0$ ). We assume a damping ratio  $\zeta = 0.05$ , which is related to the damping coefficient  $c$  as  $c = 2m\omega_1\zeta$  where  $\omega_1$  is the natural frequency of the microstructure.

Next, we show the time history response  $x(t)$  normalized to the gap width  $d$  for various values of the DC voltage and the shock amplitude. In Figure 4a, we set  $V_{DC} = 0$  and assume a shock amplitude of  $1000 g$  with duration  $T = 1.0 ms$ . As expected, the steady state value reaches the equilibrium position of zero displacement. Because the natural period of the microstructure is very small ( $0.02 ms$ ) compared to the duration of the shock load (typically it ranges from  $0.2-1.0 ms$ ), we note from Figure 4a that the microstructure experiences the shock force as a sort of static force that stays for some time then is removed. Hence, we note that the response of the microstructure looks similar to the shape of the shock force (quasi-static response). A similar conclusion can be stated for many MEMS devices, as pointed out by Srikar and Senturia [16].

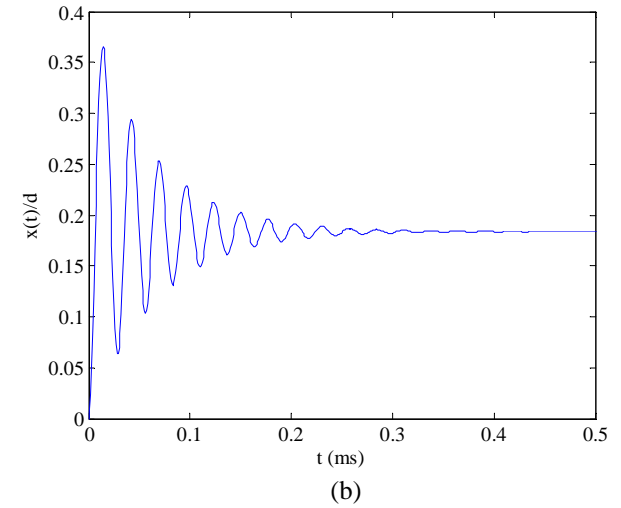
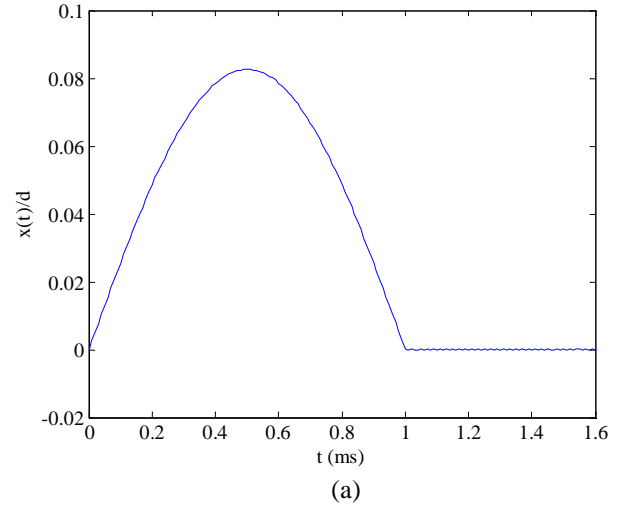


**Figure 4.** A time history for the response with (a) no electrostatic force and (b) no shock force.

Figure 4b shows the time history of the response when  $V_{DC} = 4.0 V$  and no shock applied. We note that the steady-state amplitude is near  $x(t)/d = 0.175$ . We recall here that the instability limit of a spring-mass system according to the static analysis is near  $x(t)/d = 0.33$  and according to the dynamic analysis, i.e. accounting for the transients at low damping, is 92% of the static limit, which is  $x(t)/d = 0.3$ . This corresponds to  $V_{DC} = 4.05 V$ .

Figure 5a shows the time history of the response when  $V_{DC} = 4.0V$  and a shock load applied of amplitude  $1000 g$ . It is clear that the system undergoes dynamic pull-in instability, which is characterized by a slope approaching infinity. Figure 5b shows the time history of the response when  $V_{DC} = 2.0V$  and a shock load applied of amplitude  $10000 g$ . Surprisingly, the system also undergoes dynamic pull-in instability, even though the applied voltage of  $2.0V$  is less than half the pull-in voltage of

approximately  $4.4V$ , as mentioned above. In Figure 6, we show the response of the system when  $V_{DC} = 2.0V$  and no shock force is applied. Clearly, the steady-state response is around  $x(t)/d = 0.03$ , which is very far from the pull-in instability limit  $x(t)/d = 0.3$ .

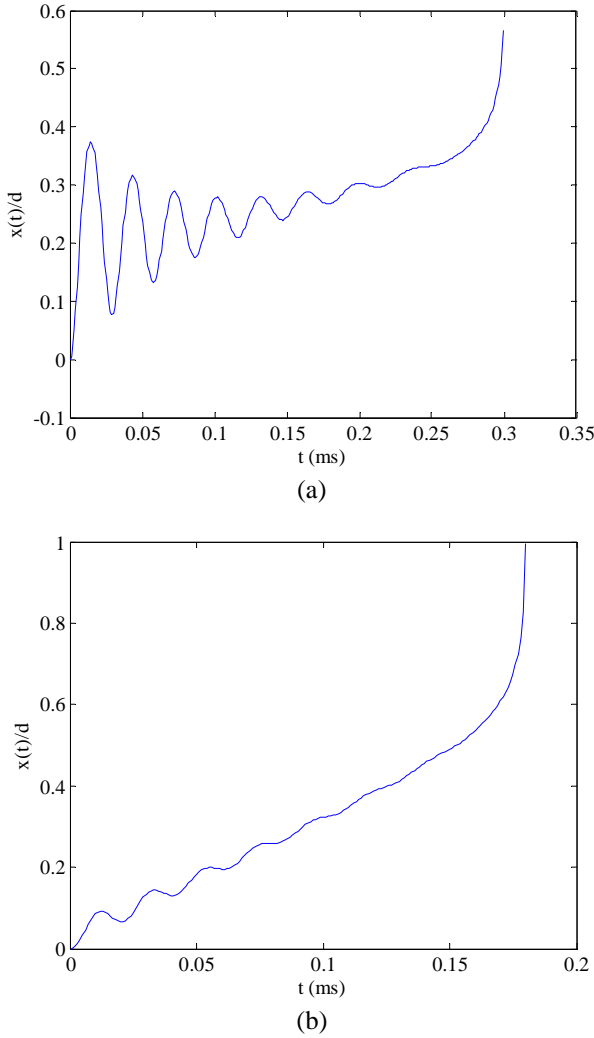


**Figure 5.** A time history showing **dynamic pull-in** when (a)  $V_{DC} = 4.0V$  and the shock amplitude is  $1000\text{ g}$  and (b)  $V_{DC} = 2.0V$  and the shock amplitude is  $10000\text{ g}$ . In both of these cases the applied voltage is less than the pull-in voltage of  $4.4V$ , but the response is unstable due to the mechanical shock.

Figures 5b and 6 indicate very interesting and important result. They show that in the presence of electrostatic forces, a stable system (for example Figure 6), which operates far from the instability threshold, can go unstable under the effect of a shock load that is even moderate in magnitude (in this case the amplitude ranges from  $1000\text{-}10000\text{ g}$ ). Therefore, in the design of a MEMS device, both the electrostatic forces and the shock forces have to be taken into account, even if the microstructure

undergoes small deflection and operates within a linear range of the electrostatic force. For example, comb-drive actuators are driven typically by small voltages. In this case, the electrostatic force is approximated to be linearly proportional to the displacements of the comb fingers. Hence in the design of these actuators, the electrostatic nonlinearity is neglected. However, as demonstrated in Figures 5b and 6, when these structures are subjected to shock, the possibility of dynamic pull-in instability becomes very high. This dynamic instability has been reported by Tanner et al. [18] as a strange mode of failure, which is characterized by contacts and overlaps among the fingers and electrodes of the parallel-plate capacitors.

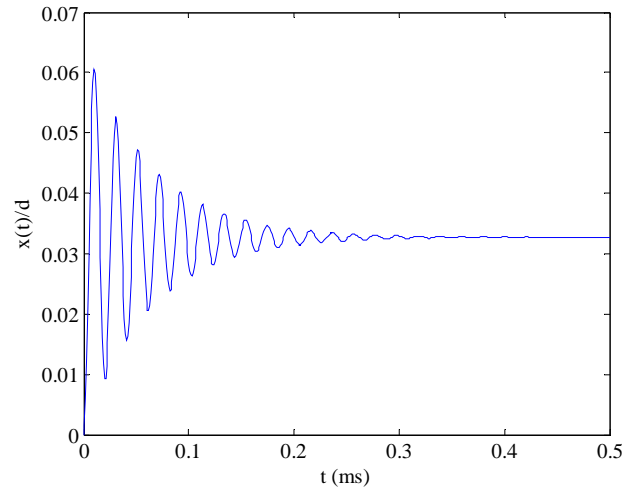


**Figure 6.** A time history of the response when  $V_{DC} = 2.0V$  and no shock force.

To better understand the influence of a shock force on the behavior of MEMS devices, we show in Figure 7 a plot for the maximum magnitude of a shock load (solid) for various values of shock amplitude as compared to the magnitude of the electrostatic force (dashed) near pull-in. We note that at low values of shock, the shock force is very small and hence it is expected to have negligible effect. However, when the shock magnitude approaches  $4000\text{ g}$ , it becomes of the same order of magnitude as the electrostatic force near pull-in. At larger values, the shock magnitude becomes much larger than the electrostatic force. Hence, at these values it is expected that the shock effect dominates over the electrostatic force. In the next figures, we investigate the influence of shock forces on the instability threshold (pull-in) of MEMS microstructures. We study shock loads of various durations and shapes and also study various damping conditions.

In Figure 8, we show a plot of the pull-in voltage of a MEMS microstructure against the shock amplitude of a half-sine pulse of duration  $1.0\text{ ms}$  (solid) and  $0.1\text{ ms}$  (dashed). We assume a damping ratio  $\zeta = 0.05$ . We note from the figure that the duration of the shock has slight effect. This is due to the fact the microstructure does not experience the shock force as

shock, as explained before, but rather as a static load. And hence, the structure does not experience any significant difference in the transient response due to those shock loads. It is worth to mention that we investigated the effect of varying the ramping rate of the DC voltage on the device and found no effect on the response. As seen from the figure, at a large shock load near  $10000g$ , the microstructure exhibits pull-in instability even if it is biased by a small value of voltage below  $0.5 V$ . We note from the figure that at low values of shock, the pull-in voltage of the short-duration shock is lower than that of the higher duration, which may look counterintuitive to what expected. This can be qualitatively understood by noting Figures 4a and 4b. Figure 4a shows that the shock load of  $T=1 ms$  reaches its peak at  $t=0.5 ms$ . From Figure 4b, we note that at this time, the response of the structure to the electrostatic force alone is almost static (no transient behavior). In the case of the shock load with  $T=0.1 ms$ , the peak will be at  $t=0.05ms$ . We can see from Figure 4b that the deflection at  $t=0.05ms$  is large and hence the transient dynamic due to the electrostatic force will be a factor in this case. At higher values of shock loads, the transient effect of the electrostatic force becomes negligible compared to the dominant effect of shock loads.

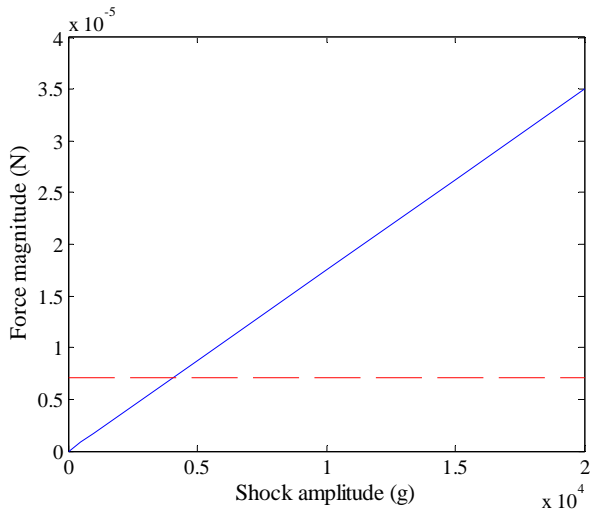


**Figure 7.** The maximum of a shock load (solid) for various values of shock amplitude as compared to the magnitude of the electrostatic force (dashed) near pull-in.

In Figure 9, we show a plot of the pull-in voltage of a MEMS microstructure against the shock amplitude of a half-sine pulse and a damping ratio  $0.05$  (solid) and  $0.7$  (dashed). We assume  $T=1.0 ms$ . Here also we note that these values of damping has nearly no effect on pull-in due to the fact the microstructure experiences the shock force as a quasi-static load.

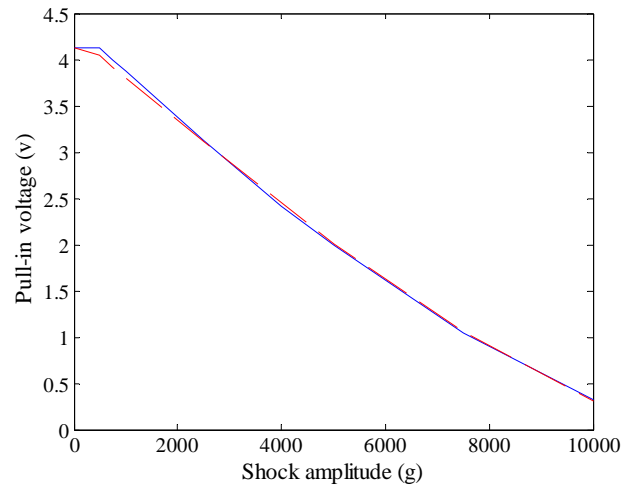


**Figure 8.** A plot of the pull-in voltage of a MEMS microstructure against the shock amplitude of a half-sine pulse of duration  $1.0 ms$  (solid) and  $0.1 ms$  (dashed).

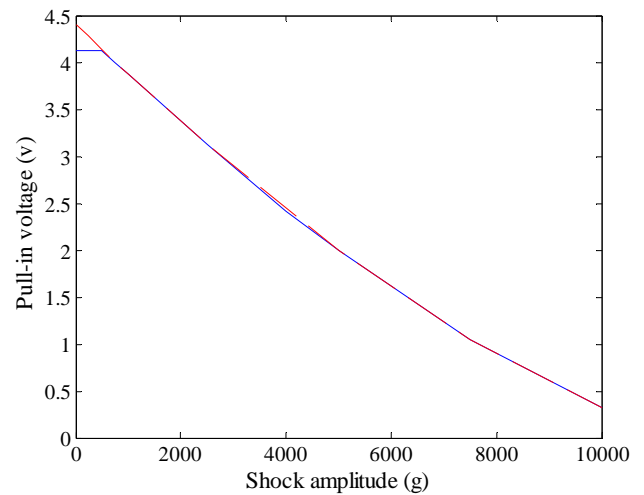


**Figure 9.** A plot of the pull-in voltage of a MEMS microstructure against the shock amplitude of a half-sine pulse and a damping ratio of  $0.05$  (solid) and  $0.7$  (dashed).

To investigate the effect of squeeze-film damping, we use the model of Starr [20], which assumes incompressible gas underneath the structure, and hence neglects the spring effect of the gas on the structure. Figure 10 shows a plot of the pull-in voltage of a MEMS microstructure against the shock amplitude of a half-sine pulse and a gas pressure of  $0.1 pa$  (solid),  $10 pa$  (dashed), and  $50 pa$  (dash-dot). The duration of the shock is set to be  $1.0 ms$ . According to this model, a gas pressure of  $10 pa$  yields a damping ratio close to  $0.05$ . Hence, we note that the results at gas pressures of  $10 pa$  and  $50 pa$  are close to those obtained in Figure 9. However, at extremely low gas pressure,  $0.1 pa$ , we note a significant decrease in the pull-in threshold.

This is because the transient behavior at very low damping near vacuum becomes a factor and the instability is a dynamic instability.

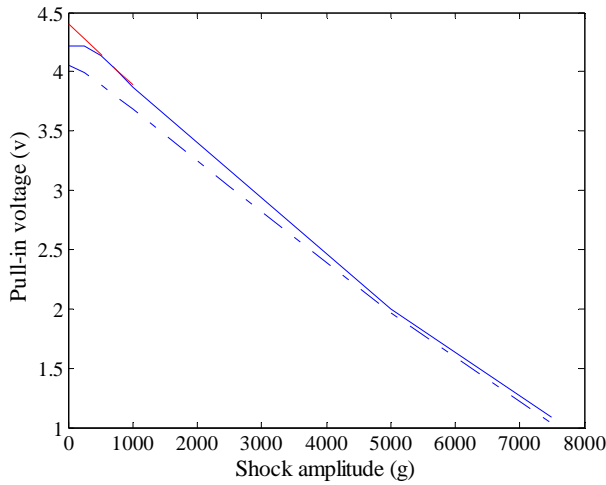


**Figure 10.** A plot of the pull-in voltage of a MEMS microstructure against the shock amplitude of a half-sine pulse and a gas pressure of  $0.1 \text{ pa}$  (solid),  $10 \text{ pa}$  (dashed), and  $50 \text{ pa}$  (dash-dot).

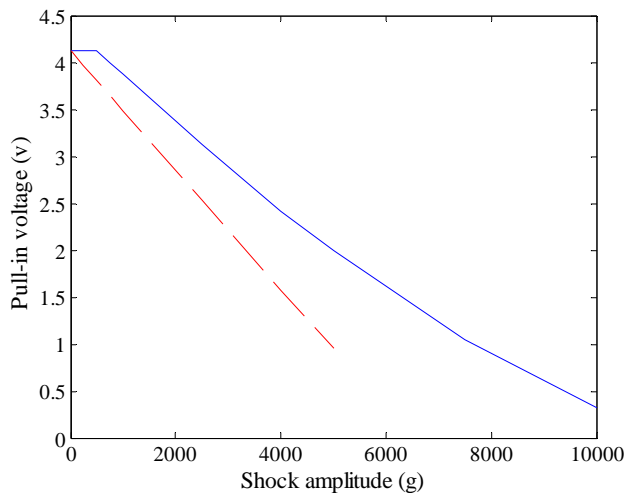


**Figure 11.** A plot of the pull-in voltage of a MEMS microstructure against the shock amplitude of a half-sine or triangle pulse (solid) and a rectangular pulse (dashed).

Next, we investigate the effect of varying the shape of the shock force. Figure 11 shows a plot of the pull-in voltage of a MEMS microstructure against the shock amplitude of a half-sine (solid), a triangle pulse (solid), and a rectangular pulse (dashed). The duration of the shock is set to be  $1.0 \text{ ms}$  and the damping ratio is set to be  $0.05$ . It turns out that there is no difference between the results of the triangle pulse and the

rectangular pulse. However, it is clear that the results of the rectangular pulse are different, in which the pull-in threshold is decreased significantly compared to the other pulses.

## SUMMARY AND CONCLUSIONS

We presented modeling and simulation of MEMS microstructures under the combination of shock loads and electric actuation and studied the influence of these forces on the dynamic pull-in instability. We investigated the effect of shock pulse shapes, shock durations and damping (linear and incompressible squeeze-film models). Our results indicate that both shock load and electrostatic force determine the instability limit pull-in of microstructures. Hence, both effects have to be accounted for in the design to ensure the reliability of MEMS devices. We considered an example of a MEMS structure with a natural period that is an order of magnitude smaller than the duration of the shock loads. Our results indicate that such microstructures experience the shock loads as quasi-static loads. We found that the shock duration, shape, and damping mechanisms have slight effect on the instability limit, except when microstructures operate at very low damping near vacuum. In this case, the pull-in is affected by the transient behavior of the structure. Our results indicate that the combination of a shock load and an electric actuation makes the instability threshold much lower than the threshold predicted considering the effect of shock alone or electric actuation alone. This conclusion helps explain many of the reported unexplained failures of MEMS devices under moderate or low shock loads.

We conclude that improved models are needed to account for the packaging effect and the various geometric details of each specific MEMS device. There are other classes of devices with low natural frequencies, such as torsional mirrors. The response of these devices is expected to be different than that presented in this paper because such structures will experience the shock load as a sudden force rather than a quasi-static load. The transient behavior in such cases will have more significance. Hence, factors such as damping, pulse duration, and pulse shape will play more crucial roles in determining the stability limits of MEMS microstructures.

## REFERENCES

1. Brown, T. G., "Harsh military environments and microelectromechanical (MEMS) devices, Proceedings of IEEE Sensors, Vol. 2, pp. 753-760, 2003.
2. Wagner, U., Franz, J., Schweiker, M., Bernhard, W., Muller-Fiedler, R., Michel, B., and Paul, O., "Mechanical reliability of MEMS-structures under shock load," Microelectronic Reliability, Vol. 41, pp. 1657-1662, 2001.
3. Tilmans, H. A. and Legtenberg, R., "Electrostatically driven vacuum-encapsulated polysilicon resonators. Part II. Theory and performance," Sensors and Actuators A, Vol. 45, pp. 67-84, 1994.

4. Osterberg, P. M. and Senturia, S. D., "M-TEST: A test chip for MEMS material property measurement using electrostatically actuated test structures," *Journal of Microelectromechanical Systems*, Vol. 6, pp. 107-118, 1997.
5. Abdel-Rahman, E. M., Younis, M. I., and Nayfeh, A. H., "Characterization of the mechanical behavior of an electrically actuated microbeam," *Journal of Micromechanics and Microengineering*, Vol. 12, pp. 795-766, 2002.
6. Younis, M. I., Abdel-Rahman, E. M., and Nayfeh, A. H., "A Reduced-order model for electrically actuated microbeam-based MEMS," *Journal of Microelectromechanical Systems*, Vol. 12, pp. 672-680, 2003.
7. Ananthasuresh, G. K., Gupta, R. K., and Senturia, S. D., "An approach to macromodeling of MEMS for nonlinear dynamic simulation," in *Proceedings of the ASME International Conference of Mechanical Engineering Congress and Exposition (MEMS)*, Atlanta, GA, pp. 401-407, 1996.
8. Krylov, S. and Maimon, R., "Pull-in dynamics of an elastic beam actuated by distributed electrostatic force," in *Proceedings of the 19th Biennial Conference in Mechanical Vibration and Noise (VIB)*, Chicago, IL, paper DETC2003/VIB-48518, 2003.
9. Younis, M. I., Abdel-Rahman, E. M., and Nayfeh, A. H., "Dynamic simulations of a novel RF MEMS switch," *NanoTech 2004: in Proc. the 7th International Conference on Modeling and Simulation of Microsystems*, Boston, pp. 287-290, 2004.
10. Cunningham, S., McIntyre, D., Carper, J., Jaramillo, P., and Tang, W. C., "Microstructures designed for shock robustness," in *Proceedings of SPIE - The International Society for Optical Engineering*, pp. 99-107, 1996.
11. Brown, T. G. and Davis, B. S., "Dynamic high-g loading of MEMS sensors: Ground and flight testing," in *Proceedings of SPIE - The International Society for Optical Engineering*, Bellingham, WA, pp. 228-235, 1998.
12. Lim, B. B., Yang, J. P., Chen, S. X., Mou, J. Q., Lu, Y., "Shock analysis of MEMS actuator integrated with HGA for operational and non-operational HDD," *Digest of the Asia-Pacific Magnetic Recording Conference*, pp. WE-P-18-01-WE-P-18-02, 2002.
13. Yee, J. K., Yang, H. H., and Judy, J. W., "Dynamic response and shock resistance of ferromagnetic micromechanical magnetometers," in *Proceedings of the Fifteenth IEEE International Conference on Micro Electro Mechanical Systems*, Las Vegas, NV, pp. 308-311, 2002.
14. Beliveau, A., Spencer, G. T., Thomas, K. A., Roberson, S. L., "Evaluation of MEMS capacitive accelerometers," *Design & Test of Computers*, Vol. 16, pp. 48 - 56, 1999.
15. Li, G. X. and Shemansky Jr., "Drop test and analysis on micro-machined structures," *Sensors and Actuators A*, Vol. 85, pp. 280-286, 2000.
16. Srikar, V. T. and S. D. Senturia, "The reliability of microelectromechanical systems (MEMS) in shock environments," *Journal of Microelectromechanical Systems*, Vol. 11, pp. 206-214, 2002.
17. Coster, J. D., Tilmans, H. C., van Beek, J. T. M., Rijks, T. G. S. M., and Puers, R., "The influence of mechanical shock on the operation of electrostatically driven RF-MEMS switches," *Journal of Micromechanics and Microengineering*, Vol. 14, pp. S49-S54, 2004.
18. Tanner, D. M., Walraven, J. A., Helgesen, K., Irwin, L. W., Smith, N. F., and Masters, N., "MEMS reliability in shock environments," in *Proceedings of the 38th IEEE Annual International Reliability Physics Symposium*, San Jose, CA, pp.129-138, 2000.
19. Senturia, S. D., *Microsystem Design*, Boston, Kulwer Academic Publishers, 2000.
20. Starr, J. B., "Squeeze-film damping in solid-state accelerometers," in *Proceeding of the IEEE Solid-State Sensor and Actuator Workshop*, Hilton Head Island, South Carolina, pp. 44-47, 1990.